

See discussions, stats, and author profiles for this publication at: <https://www.researchgate.net/publication/51801001>

Reactivities of Superoxide and Hydroperoxyl Radicals with Disubstituted Cyclic Nitrones: A DFT Study

ARTICLE *in* THE JOURNAL OF PHYSICAL CHEMISTRY A · NOVEMBER 2011

Impact Factor: 2.69 · DOI: 10.1021/jp209896n · Source: PubMed

CITATIONS

6

READS

39

2 AUTHORS, INCLUDING:



Frederick A. Villamena

The Ohio State University

88 PUBLICATIONS 1,677 CITATIONS

SEE PROFILE

Published in final edited form as:

J Phys Chem A. 2012 January 19; 116(2): 886–898. doi:10.1021/jp209896n.

Reactivities of Superoxide and Hydroperoxyl Radicals with Di-Substituted Cyclic Nitrones: A DFT Study

Shang-U Kim and Frederick A. Villamena*

Department of Pharmacology and Davis Heart and Lung Research Institute, College of Medicine, The Ohio State University, Columbus, OH, 43210

Abstract

The unique ability of nitron spin traps to detect and characterize transient free radicals by electron paramagnetic resonance (EPR) spectroscopy has fueled the development of new spin traps with improved properties. Among a variety of free radicals in chemical and biological systems, superoxide radical anion ($O_2^{\bullet-}$) plays a critical role as a precursor to other more oxidizing species such as hydroxyl radical (HO^\bullet), peroxynitrite ($ONOO^-$), and hypochlorous acid ($HOCl$), and therefore, the direct detection of $O_2^{\bullet-}$ is important. To overcome the limitations of conventional cyclic nitrones, *i.e.*, poor reactivity to $O_2^{\bullet-}$, instability of $O_2^{\bullet-}$ adduct, and poor cellular target specificity, synthesis of disubstituted nitrones has become attractive. Disubstituted nitrones offer advantages over the mono-substituted ones since they allow bi-functionalization of spin traps, therefore, accommodating all the desired spin trap properties in one molecular design. However, due to the high number of possible disubstituted analogues as candidates, a systematic computational study is needed to find leads for the optimal spin trap design for bi-conjugation. In this paper, calculation of the energetics of $O_2^{\bullet-}$ and HO_2^\bullet adducts formation from various disubstituted nitrones at PCM/B3LYP/6-31+G(d,p)//B3LYP/6-31G(d) level of theory were performed to determine the most favorable disubstituted nitrones for this reaction. In addition, our results provided general trends of radical reactivity that is dependent upon the charge densities of nitronyl-C, the position of substituents including stereoselectivities, and presence of intramolecular H-bonding interaction. Unusually high exoergic $\Delta G_{298K,aq}$'s for $O_2^{\bullet-}$ and HO_2^\bullet adducts formation were predicted for (2*S*,4*S*)-2-methyl-2,4-bis(methylcarbamoyl)-1-pyrroline *N*-oxide (**11-*cis***) and (2*R*,3*R*)-2-(dimethoxyphosphoryl)-3-(ethoxycarbonyl)-1-pyrroline *N*-oxide (**29-*trans***) with $\Delta G_{298K,aq} = -3.3$ and -9.4 kcal/mol, respectively, which are the most exoergic $\Delta G_{298K,aq}$ observed thus far for any nitrones at the level of theory employed in this study.

1. Introduction

Superoxide radical anion ($O_2^{\bullet-}$) is one of the most studied radicals in biological systems. Aerobic organisms produce $O_2^{\bullet-}$ from one-electron reduction of the triplet dioxygen molecule via enzymatic, chemical, and photochemical means, and has been the main precursor of the most reactive species (RS) species known to be formed in cellular systems, *e.g.*, hydroxyl radical (HO^\bullet), peroxynitrite ($ONOO^-$), carbonate radical anion ($CO_3^{\bullet-}$), oxidized glutathione radical anion ($GSSG^{\bullet-}$), and hypochlorous acid ($HOCl$). RS play an important role in modulating cell functions, cell signaling and immune responses^{1,2} but in unregulated concentrations, they have been implicated in the pathogenesis of cardiovascular diseases,³ cancer,⁴ neurodegeneration,⁵ and ischemia-reperfusion injury,^{6,7} to name a few.

*frederick.villamena@osumc.edu.

Supporting Information. Additional tables, thermodynamic data of all disubstituted nitrones and their respective $O_2^{\bullet-}$ and HO_2^\bullet spin adducts, and complete reference 48. This material is available free of charge via internet www.pubs.acs.org.

The formation of hydroperoxyl radical ($\text{HO} \cdot_2$) from the protonation of $\text{O}_2^{\bullet-}$ is relevant in the initiation of lipid peroxidation in cellular systems.⁸ In simple chemical systems, $\text{HO} \cdot_2$ has been shown to be produced from $\text{O}_2^{\bullet-}$ by a proton-transfer reaction from phenyl or one-electron reduction of O_2 in the presence of acid.⁹ Furthermore, the presence of small equilibrium concentration of $\text{HO} \cdot_2$ in neutral pH ($\text{p}K_a$ for $\text{HO}_2 \cdot$ is 4.8 and 4.4)^{10,11} can contribute to $\text{O}_2^{\bullet-}$ instability via a dismutation reaction with a reaction rate of $k = 9.7 \times 10^7 \text{ M}^{-1}\text{s}^{-1}$. In animal models, $\text{O}_2^{\bullet-}$ production^{12,13} is induced during ischemia and reperfusion making the detection (or sequestration for therapeutic purposes) of $\text{O}_2^{\bullet-}$ and $\text{HO}_2 \cdot$ highly important.

Nitrones are used as key synthetic precursor,¹⁴ therapeutic agent,^{15,16} and have been extensively used as reagent for the detection and characterization of free radicals¹⁷⁻²⁰ in biomedical research. Nitrone spin traps have gained popularity as reagents for the detection of radicals in the fields of fuel cell research,²¹⁻²³ nanotechnology,^{24,25} catalysis,²⁶ environmental remediation,²⁷ and photodynamic therapy.²⁸⁻³⁰ Nitrone reacts with a transient radical to form a persistent spin adduct which is detectable by electron paramagnetic resonance (EPR) spectroscopy. Among the most commonly used spin traps are DMPO (5,5-dimethyl-1-pyrroline *N*-oxide),^{31,32} EMPO (5-ethoxycarbonyl-5-methyl-1-pyrroline *N*-oxide),³³ and DEPMPO (5-diethoxyphosphoryl-5-methyl-1-pyrroline *N*-oxide),³⁴ (Figure 1) but these spin traps are limited by their slow reactivity to $\text{O}_2^{\bullet-}$ (2.0, 10.9, and $3.95 \text{ M}^{-1}\text{s}^{-1}$ in aqueous media, respectively),³⁵ short $\text{O}_2^{\bullet-}$ adduct half-life ($t_{1/2} = 1\text{-}14 \text{ min}$)³⁶ and target specificity to cellular compartments making it ambiguous to determine the source of radical production from the cell. Computational efforts over the past years led to better understanding of the chemistry of spin trapping,³⁷⁻³⁹ hence, better spin traps that incorporate most of the desired properties in one molecular design had been synthesized.^{40,41}

To date, there are three popular linker groups that have been employed for molecular tethering of cyclic nitrones, that is, ester, amide and phosphoryl groups. The main advantage of these groups is that due to their electron withdrawing properties, they can increase the electrophilic character of C-2 through inductive effect. This effect is more pronounced with the amide-substituted nitrone (AMPO) exhibiting higher reactivity to $\text{O}_2^{\bullet-}$ compared to DMPO, EMPO and DEPMPO.^{39,42} This higher reactivity of AMPO with $\text{O}_2^{\bullet-}$ is further enhanced by the presence of intramolecular H-bond interaction of the amide-H with $\text{O}_2^{\bullet-}$ at the transition state making $\text{O}_2^{\bullet-}$ hyperactive via its polarization (α -effect).⁴³ Further conjugation of the nitrone spin traps with β -cyclodextrin (CDNMPO⁴¹ and C12CDMPO⁴⁰) or calix[4]pyrrole³⁶, using amide or ester linker groups, respectively, can further enhanced the spin trapping ability of the nitrones via inductive effect or H-bonding. For example, CDNMPO, C12CDMPO, and CalixMPO (see Figure 1 and 2 for structures), gave improved rates for spin trapping of $\text{O}_2^{\bullet-}$ and $\text{O}_2^{\bullet-}$ -adduct half-lives. The spin trapping rates have been determined to be 58 (CDNMPO),⁴¹ 221 (C12CDMPO),⁴⁰ 680 (CalixMPO)³⁶ $\text{M}^{-1}\text{s}^{-1}$ and improved their respective $\text{O}_2^{\bullet-}$ -adduct half-lives ($t_{1/2}$), that is, CDNMPO (6 min), C12CDMPO (9 min), CalixMPO (25 min) in DMSO compared to DMPO alone which has a rate constant of only $2 \text{ M}^{-1}\text{s}^{-1}$ and $\text{O}_2^{\bullet-}$ -adduct half-life of 6 min in DMSO.³⁶ The biconjugation of the nitrone such as in the case C12CDMPO can provide opportunities for a nitrone design that includes target specificity to cellular compartments.

Our current goal is to systematically explore the spin trapping properties of various disubstituted nitrones and chose the most optimal design/s for disubstitution based on their energetics of reactivity with $\text{O}_2^{\bullet-}$ and $\text{HO} \cdot_2$. Through bi-functionalization of the nitrones, we would be able to integrate most of the desired spin trapping properties in one molecular design. Only a limited number of disubstituted nitrones have been synthesized over the past years, such as, C-5 diesterified nitrone (DECPO),⁴⁴ *N*-hydroxysuccinimide-, biotin-, alkylphosphonium-, Me- β -cyclodextrin-conjugated DEPMPO at C-4 (NHS-DEPMPO,

biotin-DEPMPO, Mito-DEPMPO and CD-DEPMPO, respectively),⁴⁵⁻⁴⁷ amphiphilic PBN derivative (LPBNAF),⁴⁸ and the C-5 disubstituted cyclic nitron with a long chain hydrocarbon and β -cyclodextrin (C12CDMPO)⁴⁰ (Figure 2). The aim of this work is to systematically explore, using computational approach, the thermodynamics of $\text{O}_2^{\bullet-}$ and HO_2^{\bullet} spin adduct formations from various disubstituted nitrones and find new leads for better molecular design with optimized spin trapping properties.

2. Results and discussion

2.1. Computational methods

All calculations were performed at the Ohio Supercomputer Center. For each structure, initial conformational search was performed using Spartan 04 at the MMFF level. Density functional theory (DFT)⁴⁹ was then applied to determine the optimized geometry, vibrational frequency, and single-point energy of all stationary points using Gaussian 03.⁵⁰ Single point energies were obtained at the B3LYP/6-31+G(d,p) level on the basis of the optimized B3LYP/6-31G(p) geometries. Spin adduct structures were chosen on the basis of the most stable conformer/configuration in aqueous phase via polarizable continuum model (PCM) using single-point energy calculations at the B3LYP/6-31+G(d,p) level. Spin contamination for the adduct radicals are negligible, *i.e.*, $0.75 < \langle S^2 \rangle < 0.76$. A scaling factor of 0.9806⁵¹ was used for the zero-point vibrational energy (ZPE) correction for the B3LYP geometries. Free energies were obtained from the calculated thermal and entropic corrections at 298K using the unscaled vibrational frequencies. The charge densities was obtained from a natural population analysis (NPA)⁵² at the single-point PCM/B3LYP/6-31+G(d,p).

2.2. Optimized geometries

Bond lengths and angles of optimized geometries for each disubstituted nitron and their corresponding $\text{O}_2^{\bullet-}$ and HO_2^{\bullet} adducts at the B3LYP/6-31G(d) level of theory were examined. Bond distances for C=N in nitron spin traps, the C-N in spin adducts, and the N-O in both nitrones and nitroxides, as well as the pertinent bond lengths in methylcarbamoyl, dimethoxyphosphoryl, ethoxycarbonyl, methoxy, and *N*-methylamino substituents, are in good agreement with the experimental results as shown in Table S1. The bond distances of O-O and C_{nitronyl}-O for both $\text{O}_2^{\bullet-}$ and HO_2^{\bullet} spin adducts were observed to be in the range of 1.40-1.48 Å and 1.37-1.43 Å, respectively, close to that experimentally observed for cyclic hydroperoxides of 1.46 Å.⁵³

2.3. Structural considerations

2.3.1. Disubstituted nitrones—Table 1 shows all the disubstituted nitrones that were investigated in this study. The electron-withdrawing groups (EWG) used were methylcarbamoyl, dimethoxyphosphoryl, and ethoxycarbonyl groups, while the electron-donating groups (EDG) used were, *N*-methylamino and methoxy. Disubstitution of cyclic nitron can be categorized in to three groups based on their positions, that is, geminal 3,3-, 4,4- and 5,5-disubstitution, vicinal 3,4- and 4,5-disubstitution, and the 3,5-disubstitution. In each of these categories, combinations of two types of substituents, that is, EWG-EWG, EWG-EDG, and EDG-EDG, were employed to explore the general electronic and thermodynamic effects of the position and types of functional group on the nitron. Moreover, for vicinal disubstitution, configurational isomerism was also considered, *i.e.*, *cis*- and *trans*-isomers. One or two methyl groups were included at C-5 when there is one or no EWG or EDG substituent at the C-5 position.

2.3.2. $\text{O}_2^{\bullet-}$ and HO_2^{\bullet} spin adducts—Figure 3 shows the stereoisomers of various spin adducts where R₁ and R₂ represent the substituents, and X as the radical moiety. Since

radical addition to the disubstituted nitrones results in the formation of two stereoisomers (*i.e.*, *S*- and *R*-spin adducts) on C-2, there are 2 isomers for each of the 3,3-, 4,4-, and 5,5-disubstituted nitrones, and four isomers for each of the 3,4-, 3,5-, and 4,5-disubstituted nitrones (*cis-S*-, *cis-R*-, *trans-S*-, and *trans-R*-spin adducts) (see Figure 3). Energies of reaction were calculated from the most stable conformer and/or configurations of the nitrones and their respective spin adducts. While the energetics for all the stereoisomeric adducts were calculated, only the most favorable adduct configuration for each of the nitrones are the ones presented in Table 2 (for the complete list, refer to Tables S5-S8).

2.4. Substituent effect on charge densities and energetics

2.4.1. Geminal 3,3-, 4,4- and 5,5-disubstituted spin traps—Enthalpies ($\Delta H_{298K,aq}$) and free energies ($\Delta G_{298K,aq}$) of $O_2^{\bullet-}$ and HO_2^{\bullet} reaction with various nitrones, as well as C-2 charge densities, are shown in Table 2. In general, among the geminal substituted spin traps (*i.e.*, 3,3-, 4,4- and 5,5-disubstitution), 5,5-disubstitution using two EWG's gave the highest C-2 charges compared to using mixed EDG and EWG, or two EDG's. C-2 charges were highest for spin traps **52** and **54** with 0.072e and 0.080e, respectively, where compounds **52** and **54** are characterized by a combination of -P(O)(OMe)₂ and -NHC(O)Me, and -NHC(O)Me and -CO₂Me, groups at the 5,5-position, respectively. The free energies of reaction of **52** and **54** with $O_2^{\bullet-}$ are least endoergic with $\Delta G_{298K,aq}$ of 6.9 and 5.4 kcal/mol, respectively, and are consistent with the trend in C-2 charges. The free energies of HO_2^{\bullet} reaction were in the range of -3.0 to -9.1 kcal/mol with spin traps, **50** (-9.1 kcal/mol) and **63** (-8.7 kcal/mol) to be the most favorable, which cannot be explained on the basis of C-2 charge alone. The spin traps **52** and **54**, which showed highest reactivity to $O_2^{\bullet-}$ in this category, gave intermediate free energies of reaction with HO_2^{\bullet} of -6.5 and -6.2 kcal/mol, respectively. In summary, EWG 5,5-disubstitution is more efficient for trapping $O_2^{\bullet-}$ compared to EWG 3,3 and 4,4-disubstitution while also showing thermodynamic favorability for HO_2^{\bullet} addition reaction.

2.4.2. Vicinal 3,4- and 4,5-disubstituted spin traps—The effects of vicinal disubstitution on the electronic as well as thermodynamic properties of nitrones were then investigated. No trend in C-2 charges as a function of geometric isomerism (*i.e.*, *cis* versus *trans*) was observed. For this category in general, the highest positive C-2 charge and the most favorable $\Delta G_{298K,aq}$ for $O_2^{\bullet-}$ addition reaction can be realized using 4,5-disubstitution. The C-2 charges are much lower for 3,4-disubstitution (0.001e-0.026e) compared to 4,5-disubstitution (0.031e-0.076e). The free energies of reaction of 3,4-disubstitution with $O_2^{\bullet-}$ range from 7.5 to 12.1 kcal/mol, while for 4,5-disubstitution, the $\Delta G_{298K,aq}$ range is 0.1 to 12.7 kcal/mol, with **41** ($\Delta G_{298K,aq}$ = 0.1 kcal/mol) being the most favorable in this group. Compound **41** is characterized by the presence of mixed EDG (-OMe) and EDW (-NHC(O)Me) groups at the C-4 and C-5, respectively. However, reversal of the positions, that is, having -NHC(O)Me and -OMe at the C-4 and C-5, respectively, gave less favorable $\Delta G_{298K,aq}$ of 7.4 kcal/mol and less positive C-2 charges for **44** compared to **41**, indicating the importance of C-5 substitution with an EWG.

For HO_2^{\bullet} reaction, the $\Delta G_{298K,aq}$ were calculated to be in the range of -2.3 to -6.1 kcal/mol for 3,4-disubstitution, while -4.2 to -9.4 kcal/mol for 4,5-disubstitution. Nitron **29-trans** (with -CO₂Me and -P(O)(OMe)₂ at the C-4 and C-5 positions, respectively) gave the most exoergic reactivity to HO_2^{\bullet} with a free energy of -9.4 kcal/mol. However, equally exoergic $\Delta G_{298K,aq}$ can also be observed for EDG 4,5-disubstituted spin trap with $\Delta G_{298K,aq}$ = -9.2 kcal/mol for **49**, and with mixed EDG/EWG 4,5-disubstitution gave $\Delta G_{298K,aq}$ = -9.3 kcal/mol for both **40** and **41**.

In summary, EWG substitution on C-5, regardless of the nature of substituent on C-4, imparts favorable addition to $O_2^{\bullet-}$, while the position (*i.e.*, C-4 or C-5) of EWG or EDG substitution does not have significant effects on the favorability of HO_2^{\bullet} reactivity to nitrones.

2.4.3. Disubstitution of spin traps at the 3,5 position—In general, charge densities on C-2 are highest for all the EWG substitution at the 3,5-position which range from 0.012e to 0.063e while the free energies of $O_2^{\bullet-}$ and HO_2^{\bullet} additions range from -3.3 to 10.9 kcal/mol and -2.1 to -8.9 kcal/mol, respectively. The spin trap which impart the most favorable reactivity for both $O_2^{\bullet-}$ and HO_2^{\bullet} was **11-*cis*** with -NHC(O)Me group on both C-3 and C-5 positions giving $\Delta G_{298K,aq}$'s of -3.3 and -8.9 kcal/mol for $O_2^{\bullet-}$ and HO_2^{\bullet} addition reactions, respectively. Spin trap **11-*cis*** also has also one of the highest C-2 charges of 0.062e. The $\Delta G_{298K,aq}$ of -3.3 kcal/mol observed for the $O_2^{\bullet-}$ addition to **11-*cis*** is the only exoergic reaction observed among all the disubstituted nitrones (*i.e.*, germinal and vicinal) studied in this work.

As expected, substitution of EDG's at the C-3 and C-5 positions gave C-2 charges (0.009e-0.032e) that are less positive, while the $\Delta G_{298K,aq}$ of $O_2^{\bullet-}$ addition are also more endoergic (11.3-11.5 kcal/mol) than the nitrones that have EWG. However, as previously observed with other disubstituted nitrones, the presence of EDG's as with EWG's does not affect the favorability of HO_2^{\bullet} .

2.4.4. General comparison of germinal, vicinal and 3,5-disubstitution—All the spin traps studied can be classified into five categories: Types I-IV are spin traps with EWG and/or EDG substitution on C-5 while Type V are the ones with EWG and/or EDG substitution on C-3 and C-4 except on C-5 (see Table 3). As shown in Figure 4a, a general trend can be observed in which amide substitution at C-5 (regardless of the nature and position of the other substituents) imparts the greatest favorability for $O_2^{\bullet-}$ addition with ester and phosphoryl groups showing similar energetics but lower than the amide. This trend is comparable to the previously predicted order of reactivity for mono-substituted nitrones to $O_2^{\bullet-}$ showing the amide to be the most favorable, that is, AMPO, EMPO, and DEPMPO with $\Delta G_{298K,aq}$'s of 6.1, 9.7, and 14.7 kcal/mol, respectively.

For Types I and II spin traps, one can also observe an increase in favorability of $O_2^{\bullet-}$ adduct formation in the presence of *any* EWG at the C-5 position (Figure 4a). The favorability of $O_2^{\bullet-}$ addition to Type I and II spin traps tends to be higher than the Types III – V spin traps where the C-5 is substituted with *any* EDG or without substitution in the case of Type V. However, there is no global correlation in the energetics of reactivity to HO_2^{\bullet} *versus* the type of spin traps (Figure 4b) can be observed. The average $\Delta G_{298K,aq}$ for Types I through IV spin traps are comparable, except for the least favorable Type V spin traps. Therefore, substitution of an EWG at C-5 does not improve the energetics of HO_2^{\bullet} adduct formation, and that Type V spin traps are not ideal designs for HO_2^{\bullet} trapping.

2.5. Structural studies of favored spin traps

2.5.1. Favored spin traps for $O_2^{\bullet-}$ —As shown in Table 2, free energies of $O_2^{\bullet-}$ addition to nitrones are mostly endoergic ranging from 0.1 to 15.6 kcal/mol, with the exception of **11-*cis***- $O_2^{\bullet-}$ formation with an exoergic $\Delta G_{298K,aq} = -3.3$ kcal/mol (Figure 5). Additionally, the five spin traps with the lowest endoergic reactivity to $O_2^{\bullet-}$ have amide substitution at the C-5, that is, **44-*cis*** ($\Delta G_{298K,aq} = 0.1$ kcal/mol), **20-*trans*** ($\Delta G_{298K,aq} = 2.8$ kcal/mol), **31-*trans*** ($\Delta G_{298K,aq} = 3.0$ kcal/mol), **32-*cis*** ($\Delta G_{298K,aq} = 3.1$ kcal/mol), and **32-*trans*** ($\Delta G_{298K,aq} = 3.2$ kcal/mol) which are all more favorable compared to AMPO with $\Delta G_{298K,aq} = 6.1$ kcal/mol³⁹ suggesting additional inductive contributions via substitution at

the C-3 and C-4 positions. It should be noted that AMPO gave high experimental rate of reaction with $O_2^{\bullet-}$ and we can predict that the spin traps mentioned above may exhibit the same or more improved spin trapping rates compared to AMPO. All of the $O_2^{\bullet-}$ adducts of the nitrones above exhibited intramolecular $NH_{amide} \cdots O_{superoxide}$ bonding with a H-bond distance of 1.50-1.66 Å. Only **11-cis-S-O₂^{•-}** exhibits two $NH_{amide} \cdots O_{superoxide}$ H-bonding interaction giving H-bond distances of 1.61 and 1.66 Å, and this could account for its high exoergic $\Delta G_{298K,aq}$ of formation. The C-2 charge density in **11-cis** is comparable to that of AMPO (0.062 e) which could also be a contributing factor for the enhanced reactivity towards $O_2^{\bullet-}$. The 4,5-disubstituted nitrones, **32-cis** and **31-trans** gave higher charge densities for C-2 with 0.076e and 0.062e, respectively, compared to that of AMPO. In spite of the higher positivity on C-2 for **32-cis** and **31-trans** than **11-cis**, their endoergic $\Delta G_{298K,aq}$ for $O_2^{\bullet-}$ reaction compared to that of **11-cis** indicates that the extensive intramolecular H-bonding in **11-cis** plays a major role in facilitating radical addition. Strong H-bonding interaction between the amide-H and $O_2^{\bullet-}$ in the transition state results in the polarization of $O_2^{\bullet-}$ spin density distribution as previously demonstrated.³⁹ This observation parallels the one made for nitrone conjugate of calix[4]pyrrole (CalixMPO) showing extensive H-bonding interactions with $O_2^{\bullet-}$.³⁶ In summary, substitution at the C-5 position by amide group increases spin-trap reactivity to $O_2^{\bullet-}$ compared to other functional groups. Favorable free energies for the formation of $O_2^{\bullet-}$ adducts of **20-trans**, **21-trans**, and **41-cis** (see above for $\Delta G_{298K,aq}$'s) were observed in spite of the presence of EDG substituents at the C-3 and C-4 positions in these nitrones.

2.5.2. Favored spin traps for HO_2^{\bullet} —As shown in Table 2, the addition of HO_2^{\bullet} to disubstituted nitrones are mostly exoergic which range from -0.2 to -9.4 kcal/mol (except for **10-R-O₂H** with endoergic $\Delta G_{298K,aq} = 0.4$ kcal/mol). In Figure 6, **29-trans** showed the most favorable reactivity to HO_2^{\bullet} with $\Delta G_{298K,aq} = -9.4$ kcal/mol. Additionally, a relatively favorable reactivity to HO_2^{\bullet} was observed for the 4,5-disubstituted nitrones, **40-trans**, **41-cis** and **44-trans** all giving similar $\Delta G_{298K,aq}$'s of -9.3 kcal/mol. These values are more exoergic compared to those observed for AMPO ($\Delta G_{298K,aq} = -1.6$ kcal/mol) and DEPMPO ($\Delta G_{298K,aq} = -4.8$ kcal/mol). The charge densities of nitronyl-C are as follows: **29-trans** (0.042e), **40-trans** (0.044e), **41-cis** (0.041e), and **44-trans** (0.023e) which are lower than those for AMPO, but are mostly comparable to that of DEPMPO. In spite of the absence of EWG in **44-trans** at the C-5 position, this nitrone still exhibited an exoergic $\Delta G_{298K,aq}$. Therefore, the favorability of HO_2^{\bullet} addition to certain nitrones does not follow the same trend observed for $O_2^{\bullet-}$ addition. However, these results are consistent with our previous findings³⁹ in which we have shown poor correlation between the C-2 charge densities and $\Delta G_{298K,aq}$ of HO_2^{\bullet} addition suggesting that electrostatic effects play a minor role in nitrone reactivity with HO_2^{\bullet} .

2.6. Comparison of energetics of favored spin traps, 11 and 29, with mono-substituted spin traps.

2.6.1. Thermodynamic considerations for $O_2^{\bullet-}$ and HO_2^{\bullet} adduct formation—

Figure 7a shows correlation between the C-2 charge densities and free energies of reaction with $O_2^{\bullet-}$ and HO_2^{\bullet} for **11-cis** and **29-trans** along with DMPO, AMPO, EMPO, CPCOMPO, DEPMPO, and CalixMPO.³⁶ In spite that **11-cis** exhibits comparable C-2 charge density with AMPO and higher charge density than CalixMPO, **11-cis** gave a more exoergic reactivity to $O_2^{\bullet-}$ compared to AMPO and CalixMPO. Also the presence of strong H-bonding interactions with $NH_{amide} \cdots O_{superoxide}$ distances of 1.61-1.66 Å (see Figure 5) are significantly stronger than the $NH_{pyrrole} \cdots O_{superoxide}$ distances observed in the CalixMPO- $O_2^{\bullet-}$ adduct of 1.80-1.88 Å. These results suggest that the **11-cis** reactivity to $O_2^{\bullet-}$ is a synergistic effect between the strong intramolecular H-bonding interaction and electrostatic effect with the former being more dominant.

As shown in Figure 7b, correlation of charge densities with free energies of reaction to HO_2^\bullet for **29-trans** and other known nitrones does not follow the same trend observed for the formation of $\text{O}_2^{\bullet-}$ adducts. **29-trans** exhibits lower C-2 charge density and gave highly exoergic $\Delta G_{298\text{K},\text{aq}}$ compared to DEPMPO, CalixMPO, and AMPO.

2.6.2. Kinetic considerations for $\text{O}_2^{\bullet-}$ and HO_2^\bullet adduct formation—The relative $\Delta H_{298\text{K},\text{aq}}$ and $\Delta G_{298\text{K},\text{aq}}$ of the complexes, transition states and the most preferred $\text{O}_2^{\bullet-}$ and HO_2^\bullet adducts for **11-cis** and **29-trans** are shown in Table 4, while Figure 8 shows their respective optimized structures. The energy barrier for **11-cis-S-O}_2^{\bullet-}** adduct formation was $\Delta G_{298\text{K},\text{aq}}^\ddagger = 14.4$ kcal/mol which is lower than that previously calculated for CalixMPO and AMPO with $\Delta G_{298\text{K},\text{aq}}^\ddagger = 17.5$ and 17.4 kcal/mol, respectively (see Table S2). Examination of the $[\text{11-cis-S-O}_2^{\bullet-}]^\ddagger$ structure reveals that the $\text{O}_2^{\bullet-}$ exhibits strong H-bond interaction with the two amide-H's at C-3 and C-5 positions prior to the C-O bond formation. This observation is similar to that observed for the $[\text{AMPO-O}_2^{\bullet-}]^\ddagger$ structure in which the calculated lower energy barrier for $\text{O}_2^{\bullet-}$ addition to AMPO was previously rationalized to be due to the strong H-bonding interaction between amide-H and $\text{O}_2^{\bullet-}$ in the TS. The “anchoring” of $\text{O}_2^{\bullet-}$ to the amide-H results in the polarization of the $\text{O}_2^{\bullet-}$ electron distribution. The $\Delta G_{298\text{K},\text{aq}}^\ddagger$ (14.4 kcal/mol) and $\Delta G_{298\text{K},\text{aq}}$ (−3.3 kcal/mol) for **11-cis-S-O}_2^{\bullet-}** values are significantly more favorable compared to AMPO with $\Delta G_{298\text{K},\text{aq}}^\ddagger$ and $\Delta G_{298\text{K},\text{aq}}$ of 17.4 and 6.1 kcal/mol, respectively, but comparable to that of CalixMPO with $\Delta G_{298\text{K},\text{aq}}^\ddagger = 17.5$ and $\Delta G_{298\text{K},\text{aq}} = -2.1$ kcal/mol, indicating that $\text{O}_2^{\bullet-}$ addition to **11-cis** can also be both thermodynamically and kinetically favorable, and can translate to a much high experimental rate constants comparable to CalixMPO addition to $\text{O}_2^{\bullet-}$. The TS structure gave charge distributions of −0.62e and −0.37e for internal and external oxygens, respectively, and the spin densities were calculated to be 0.08e (internal O) and 0.22e (external O). Moreover, the strong H-bonding interaction between the amide-H's and $\text{O}_2^{\bullet-}$ allows $\text{O}_2^{\bullet-}$ polarization and eventual facile addition to the nitron.

The energy barrier for $[\text{29-trans-S-O}_2\text{H}]^\ddagger$ was also predicted to be $\Delta G_{298\text{K},\text{aq}}^\ddagger = 15.7$ kcal/mol which is lower than the $\Delta G_{298\text{K},\text{aq}}^\ddagger$ observed for $[\text{DEPMPO-O}_2\text{H}]^\ddagger$ (17.3 kcal/mol) but comparable to that of $[\text{EMPO-O}_2\text{H}]^\ddagger$ (15.9 kcal/mol) (see Table S3). The calculated spin densities for the HO_2^\bullet atoms are 0.52e for the distal O and 0.17e on the proximal O relative to H, indicating that some electron transfer occurs from the HO_2^\bullet to the nitron in the TS structure. The TS structure of $[\text{29-trans-S-O}_2\text{H}]^\ddagger$ shows intramolecular H-bonding interaction between nitronyl-O and hydroperoxyl-H with H-bond distance of 2.03 Å. This predicted interactions play a significant role in stabilizing the TS structures and, therefore, for more facile formation of the adduct.

2.7. Thermodynamic comparison of **11** with di- and tri-amide substituted nitrones for $\text{O}_2^{\bullet-}$ spin adduct formation

To further confirm the effect of the presence of H-bond donors on the favorability of adduct formation, the energetics using non-alkylated amide (−C(O)NH₂) substitution was then explored. The energetics of $\text{O}_2^{\bullet-}$ adduct formations from 3,5-*cis*-DiAMPO, 4,5-*cis*-DiAMPO, and 3,4,5-*cis*-TriAMPO substituted nitrones were calculated and are shown in Figure 9a-c. The $\Delta G_{298\text{K},\text{aq}}$'s of formation for 3,5-*cis*-DiAMPO- $\text{O}_2^{\bullet-}$, 4,5-*cis*-DiAMPO- $\text{O}_2^{\bullet-}$, and 3,4,5-*cis*-TriAMPO- $\text{O}_2^{\bullet-}$ were −3.0, −1.6, and −2.0 kcal/mol, respectively, and the intramolecular NH_{amide} $^{\text{L}}\text{O}_{\text{superoxide}}$ H-bond distances are in the range of 1.62 – 1.79 Å, with the DiAMPO- $\text{O}_2^{\bullet-}$ analogues giving comparable distances to that predicted for **11-cis-S-O}_2^{\bullet-}** adduct. It is interesting to note that the presence of two intramolecular NH_{amide} $^{\text{L}}\text{O}_{\text{superoxide}}$ H-bond in DiAMPO- $\text{O}_2^{\bullet-}$ only follows **11-cis** but not the 4,5-disubstituted, **32-cis**, (which only has one H-bonding interaction) due perhaps to repulsive effect between the two adjacent *N*-methyl groups, thus preventing one amide group to tilt.

The 4,5-*cis*-DiAMPO and 3,4,5-*cis*-TriAMPO nitrones gave less exoergic free energies compared to 3,5-DiAMPO further demonstrating that the 3,5-mono-*N*-alkyl substitution is the optimal amide design for facile $O_2^{\bullet-}$ addition. Moreover, the effect of *N,N*-dialkylation of the amide substituent using -C(O)NMe₂ groups (Figure 9d-e) on the energetics of $O_2^{\bullet-}$ addition was also explored, and results show highly endoergic $\Delta G_{298K,aq} = 13.7$ and 15.4 kcal/mol indicating the importance of H-bond in facilitating adduct formation.

Conclusion—Thermochemistries of $O_2^{\bullet-}$ and HO_2^{\bullet} spin adduct formations from various disubstituted nitrones were calculated at the PCM(water)/B3LYP/6-31+G(d,p)//B3LYP/6-31G(d) level of theory. General trends in spin trap reactivity indicate the need of an EWG (specifically an amide group) at the C-5 position resulting in higher positive charge on C-2, and exoergic $O_2^{\bullet-}$ spin adduct formation, but the trend of favorability for HO_2^{\bullet} adduct formation is not consistent with that observed for $O_2^{\bullet-}$, due to the electrophilic nature of HO_2^{\bullet} addition. The presence of an amide group allows the formation of strong intramolecular H-bonding interaction which plays a critical role for facile $O_2^{\bullet-}$ addition. The disubstituted nitrone of **11-cis** shows the most exoergic $\Delta G_{298K,aq}$ with $O_2^{\bullet-}$ compared to all disubstituted nitrones considered in this study. The highest reactivity to HO_2^{\bullet} was observed for **29-trans** which is characterized by the stabilization of the TS structure due to the presence of intramolecular H-bonding. This study paves the way for the design of mono-*N*-substituted amide nitrones (**11-cis**) as parent molecule providing high reactivity to $O_2^{\bullet-}$. Upon molecular tethering with other groups, **11-cis** can improve adduct stability and ultimately be made as multifunctional spin traps. Synthesis of **11** in our laboratory is in progress and will be reported in due course.

Supplementary Material

Refer to Web version on PubMed Central for supplementary material.

Acknowledgments

This publication was made possible by Grant RO1 HL81248 from the NIH National Heart, Lung, and Blood Institute. This work was supported by an allocation of computing time from the Ohio Supercomputer Center.

References

- (1). Halliwell, B.; Gutteridge, JMC. Free Radicals in Biology and Medicine. x. Oxford University Press; New York: 2007.
- (2). Finkel T, Holbrook NJ. Nature. 2000; 408:239. [PubMed: 11089981]
- (3). Cohen RA, Tong X. J. Cardiovasc. Pharmacol. 2010; 55:308. [PubMed: 20422735]
- (4). Benz CC, Yau C. Nat. Rev. Cancer. 2008; 8:875. [PubMed: 18948997]
- (5). Sayre LM, Perry G, Smith MA. Chem. Res. Toxicol. 2008; 21:172. [PubMed: 18052107]
- (6). Zweier JL, Talukder HMA. Cardiovasc. Res. 2006; 70:181. [PubMed: 16580655]
- (7). Zweier, JL.; Villamena, FA. Chemistry of Free Radicals in Biological Systems. In: Kukin, ML.; Fuster, V., editors. Oxidative Stress and Cardiac Failure. Futura Publishing; Armonk, NY: 2003. p. 67
- (8). Cheng Z, Li Y. Chem. Rev. 2007; 107:748. [PubMed: 17326688]
- (9). Sawyer DT, Chiericato G Jr. Angelis CT, Nanni EJ Jr. Tsuchiya T. Anal. Chem. 1982; 54:1720.
- (10). Behar D, Czapski G, Rabani J, Dorfman LM, Schwarz HA. J. Phys. Chem. 1970; 74:3209.
- (11). Czapski G, Bielski BHJ. J. Phys. Chem. 1963; 67:2180.
- (12). Zweier JL, Flaherty JT, Weisfeldt ML. Proc. Natl. Acad. Sci. U. S. A. 1987; 84:1404. [PubMed: 3029779]
- (13). Zweier JL, Kuppusamy P, Williams R, Rayburn BK, Smith D, Weisfeldt ML, Flaherty JT. J. Biol. Chem. 1989; 264:18890. [PubMed: 2553726]

- (14). Feuer, H., editor. Nitrile Oxides, Nitrones, and Nitronates in Organic Synthesis: Novel Strategies in Synthesis. 2nd ed.. John Wiley and Sons, Inc.; Hoboken, NJ: 2008.
- (15). Floyd RA, Kopke RD, Choi C-H, Foster SB, Doblas S, Towner RA. Free Radical Biol. Med. 2008; 45:1361. [PubMed: 18793715]
- (16). Floyd RA, Towner RA, He T, Hensley K, Maples KR. Free Radical Biol. Med. 2011; 51:931. [PubMed: 21549833]
- (17). Villamena FA, Zweier JL. Antioxidant Redox Signaling. 2004; 6:619.
- (18). Rosen, GM.; Britigan, BE.; Halpern, HJ.; Pou, S. Free Radicals: Biology and Detection by Spin Trapping. Oxford University Press; New York: 1999.
- (19). Rhodes, CJ., editor. Toxicology of the Human Environment. The Critical Role of Free Radicals. Taylor and Francis; London: 2000.
- (20). Janzen EG. Acct. Chem. Res. 1971; 4:31.
- (21). Bosnjakovic A, Kadirov MK, Schlick S. Res. Chem. Intermed. 2007; 33:677.
- (22). Bosnjakovic A, Schlick S. J. Phys. Chem. B. 2006; 110:10720. [PubMed: 16771319]
- (23). Danilczuk M, Bosnjakovic A, Kadirov MK, Schlick S. J. Power Sources. 2007; 172:78.
- (24). Dodd NJ, Jha AN. Photochem. Photobiol. 2011; 87:632. [PubMed: 21244435]
- (25). Ionita P, Conte M, Gilbert BC, Chechik V. Org. Biomol. Chem. 2007; 5:3504. [PubMed: 17943210]
- (26). Fu H, Zhang L, Zhang S, Zhu Y, Zhao J. J. Phys. Chem. B. 2006; 110:3061. [PubMed: 16494309]
- (27). Xiao G, Wang X, Li D, Fu X. J. Photochem. Photobiol., A. 2008; 193:213.
- (28). Mroz P, Pawlak A, Satti M, Lee H, Wharton T, Gali H, Sarna T, Hamblin MR. Free Radical Biol. Med. 2007; 43:711. [PubMed: 17664135]
- (29). Rajendran M, Inbaraj JJ, Gandhidasan R, Murugesan R. J. Photochem. Photobiol., A. 2006; 182:67.
- (30). Zeng Z, Zhou J, Zhang Y, Qiao R, Xia S, Chen J, Wang X, Zhang B. J. Phys. Chem. B. 2007; 111:2688. [PubMed: 17315917]
- (31). Bonnett R, Brown RFC, Clark VM, Sutherland IO, Todd A. J. Chem. Soc. 1959; 2094
- (32). Finkelstein E, Rosen GM, Rauckman EJ. J. Am. Chem. Soc. 1980; 102:4994.
- (33). Olive G, Mercier A, Le Moigne F, Rockenbauer A, Tordo P. Free Radical Biol. Med. 2000; 28:403. [PubMed: 10699752]
- (34). Frejaville C, Karoui H, Tuccio B, le Moigne F, Culcasi M, Pietri S, Lauricella R, Tordo P. J. Chem. Soc., Chem. Commun. 1994; 1793
- (35). Lauricella R, Allouch A, Roubaud V, Bouteiller J-C, Tuccio B. Org. Biomol. Chem. 2004; 2:1304. [PubMed: 15105920]
- (36). Kim S-U, Liu Y, Nash KM, Zweier JL, Rockenbauer A, Villamena FA. J. Am. Chem. Soc. 2010; 132:17157.
- (37). Boyd SL, Boyd RJ. J. Phys. Chem. 1994; 98:11705.
- (38). Villamena FA. J. Phys. Chem. A. 2009; 113:6398. [PubMed: 19425559]
- (39). Villamena FA, Xia S, Merle JK, Lauricella R, Tuccio B, Hadad CM, Zweier JL. J. Am. Chem. Soc. 2007; 129:8177. [PubMed: 17564447]
- (40). Han Y, Liu Y, Rockenbauer A, Zweier JL, Durand G, Villamena FA. J. Org. Chem. 2009; 74:5369. [PubMed: 19530689]
- (41). Han Y, Tuccio B, Lauricella R, Villamena FA. J. Org. Chem. 2008; 73:7108. [PubMed: 18707169]
- (42). Villamena FA, Rockenbauer A, Gallucci J, Velayutham M, Hadad CM, Zweier JL. J. Org. Chem. 2004; 69:7994. [PubMed: 15527282]
- (43). Field SM, Villamena FA. Chem. Res. Toxicol. 2008; 21:1923. [PubMed: 18816073]
- (44). Karoui H, Clement J-L, Rockenbauer A, Siri D, Tordo P. Tetrahedron Lett. 2004; 45:149.
- (45). Hardy M, Bardelang D, Karoui H, Rockenbauer A, Finet J-P, Jicsinszky L, Rosas R, Ouari O, Tordo P. Chem.--Eur. J. 2009; 15:11114. [PubMed: 19760720]

- (46). Hardy M, Rockenbauer A, Vasquez-Vivar J, Felix C, Lopez M, Srinivasan S, Avadhani N, Tordo P, Kalyanaraman B. *Chem. Res. Toxicol.* 2007; 20:1053. [PubMed: 17559235]
- (47). Hardy M, Ouari O, Charles L, Finet J-P, Iacazio G, Monnier V, Rockenbauer A, Tordo P. *J. Org. Chem.* 2005; 70:10426. [PubMed: 16323853]
- (48). Durand G, Poeggeler B, Boeker J, Raynal S, Polidori A, Pappolla MA, Hardeland R, Pucci B. *J. Med. Chem.* 2007; 50:3976. [PubMed: 17649989]
- (49). Labanowski, JW.; Andzelm, J. *Density Functional Methods in Chemistry*. Springer; New York: 1991.
- (50). Frisch, MJ., et al. Gaussian, Inc. Wallingford, CT: 2004.
- (51). Scott AP, Radom L. *J. Phys. Chem. A.* 1996; 100:16502.
- (52). Reed AE, Curtiss LA, Weinhold F. *Chem. Rev.* 1988; 88:899.
- (53). Alini S, Citierio A, Farina A, Fochi MC, Malpezzi L. *Acta Crystallogr., Sect. C: Cryst. Struct. Commun.* 1998; C54:1000.

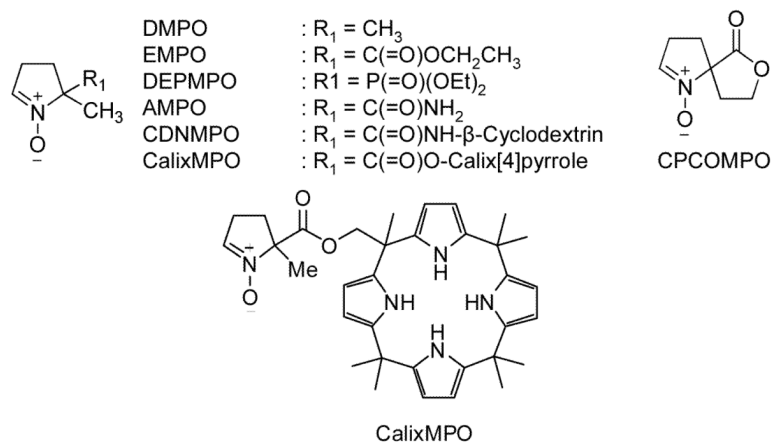


Figure 1.
Structures of cyclic nitron spin traps

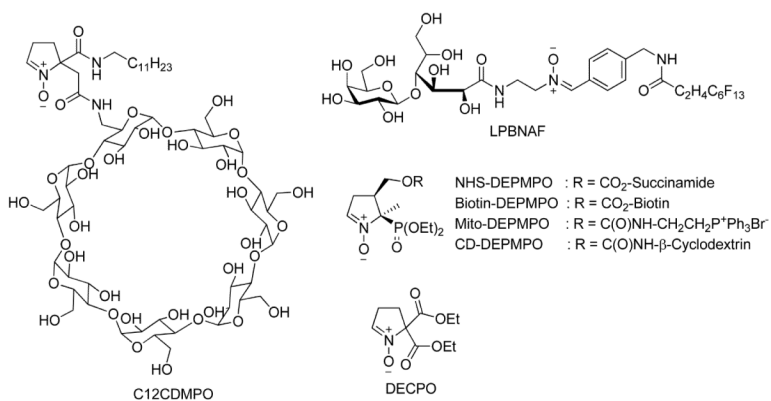


Figure 2.
Structures of disubstituted nitron spin traps

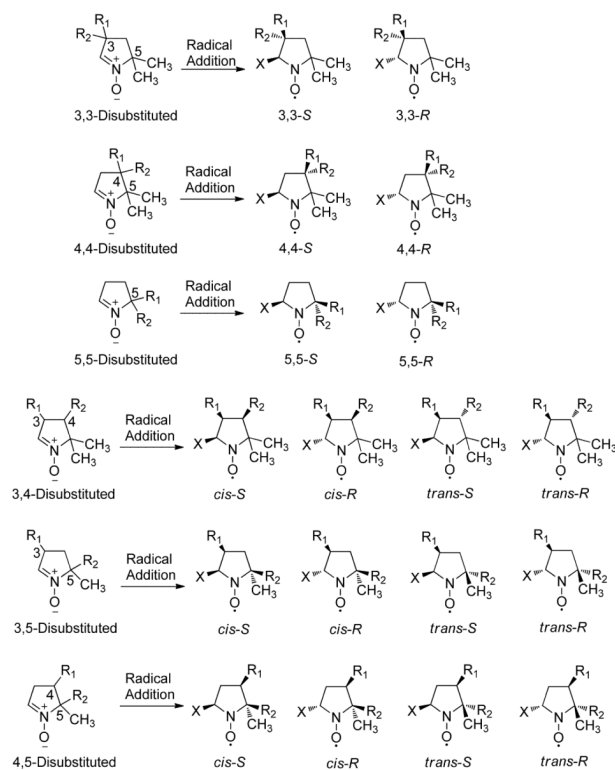


Figure 3. Stereoisomers of spin adducts from 3,3-, 4,4-, 5,5-, 3,4-, 4,5-, and 5,5-disubstituted nitrones (R_1 and R_2 represent substituents, and X as radical moiety).

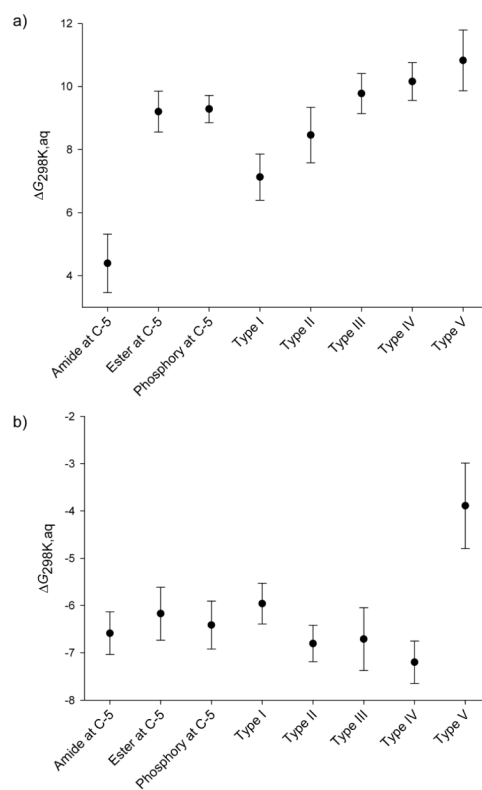
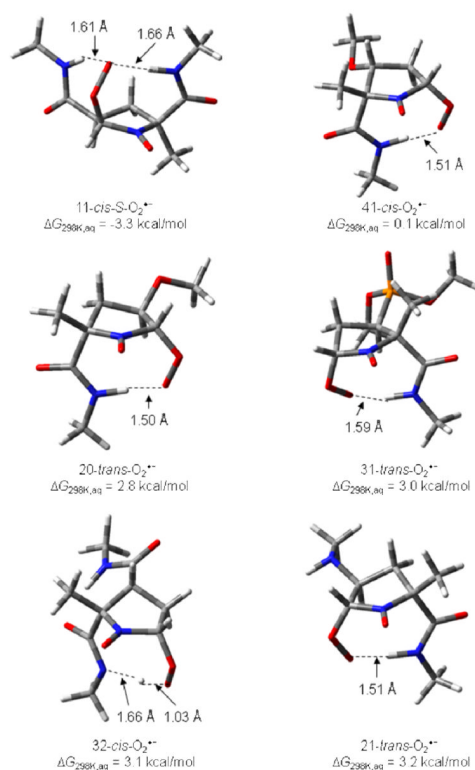


Figure 4. Average $\Delta G_{298K,aq}$ (in kcal/mol) for (a) $O_2^{\bullet-}$ and (b) HO_2^{\bullet} spin adduct formations for various types of disubstituted nitrones. (see Table 3 for the description of the various types).

**Figure 5.**

Optimized structures of the most favorable HO_2^{\bullet} adduct including $\Delta G_{298\text{K,aq}}$ and bond lengths at the PCM/B3LYP/6-31+G(d,p)//B3LYP/6-31G(d) level of theory.

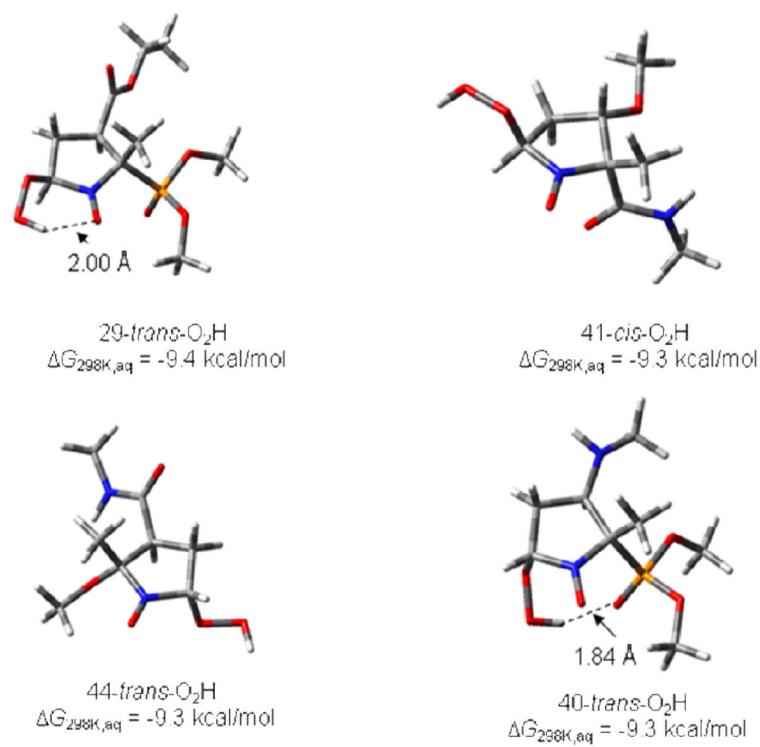


Figure 6. Optimized structures of the most favorable HO₂[•] adduct including $\Delta G_{298K, aq}$ and bond lengths at the PCM/B3LYP/6-31+G(d,p)//B3LYP/6-31G(d) level of theory.

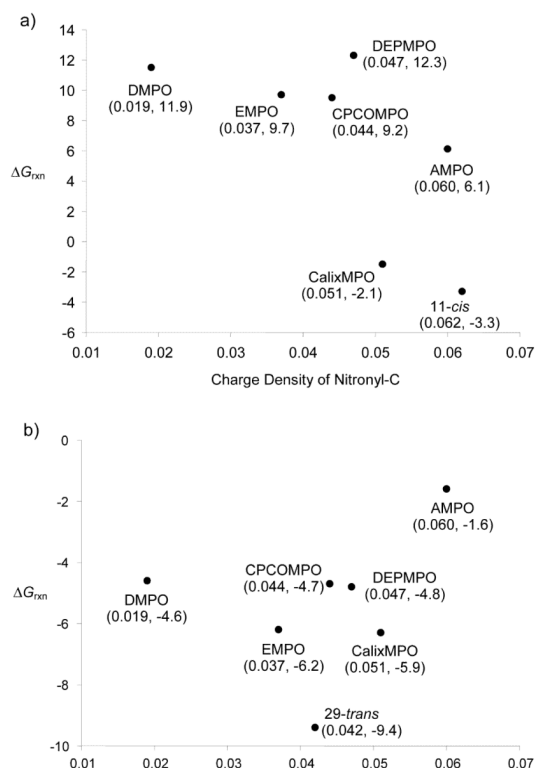


Figure 7. Correlation of charge densities with free energies of (a) $O_2^{\bullet-}$ and (b) HO_2^{\bullet} adduct formations for **11-cis** and **29-trans** relative to other nitrones. Values in parentheses are charge densities (left, in e) and $\Delta G_{298K,aq}$ (right, in kcal/mol).

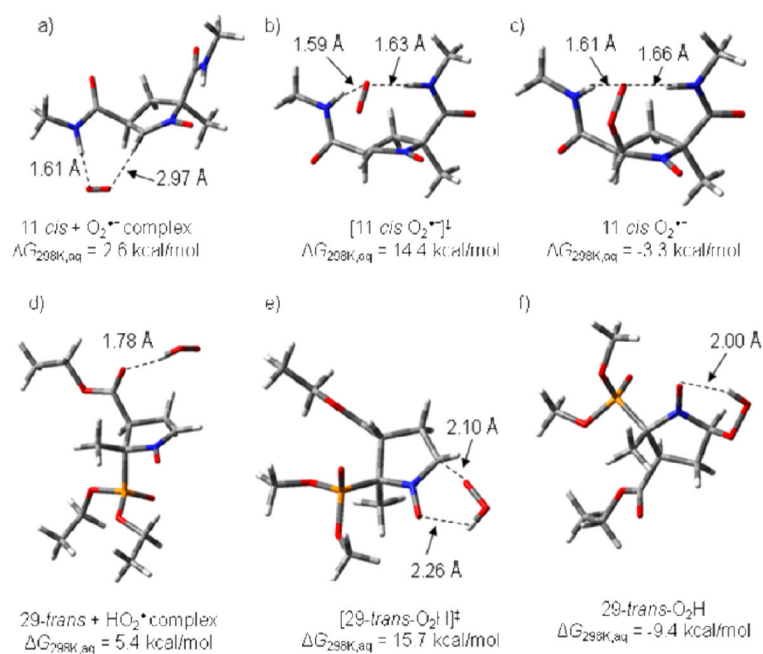
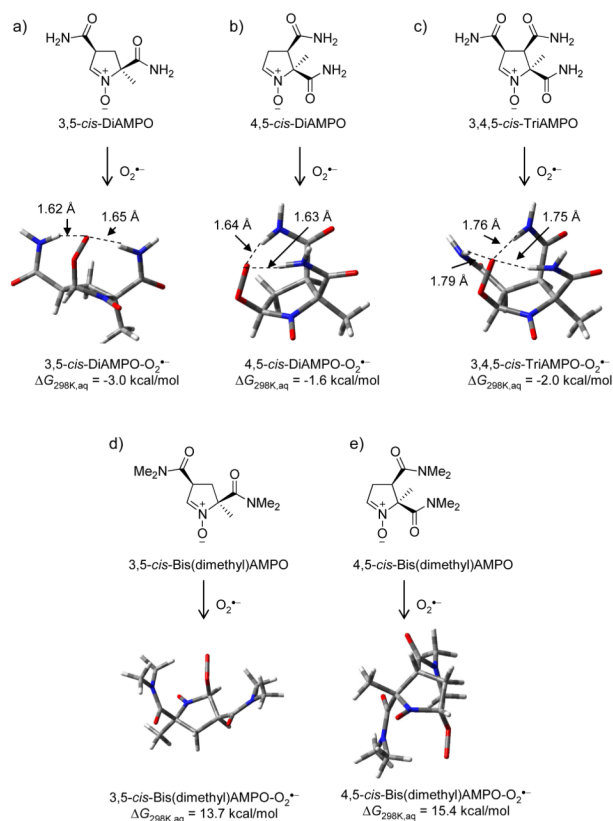


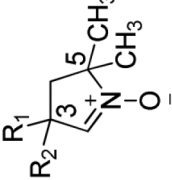
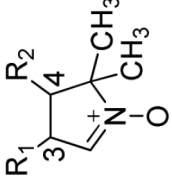
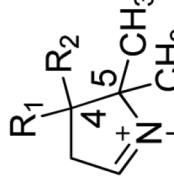
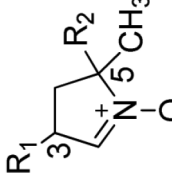
Figure 8. Optimized structures for complexes (a and d); transition states (b and e); and spin adducts (c and f) of 11-*cis* with $O_2^{\bullet-}$ and 29-*trans* with HO_2^{\bullet} including $\Delta G_{298K,aq}$ and bond lengths at the PCM/B3LYP/6-31+G(d,p)//B3LYP/6-31G(d) level of theory.

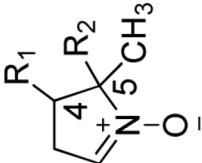
**Figure 9.**

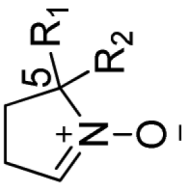
Optimized structures for $O_2^{\bullet-}$ adducts of (a) 3,5-*cis*-DiAMPO, (b) 4,5-*cis*-DiAMPO, (c) 3,4,5-*cis*-TriAMPO, (d) 3,5-*cis*-Bis(dimethyl)AMPO, and (e) 4,5-*cis*-Bis(dimethyl)AMPO, including $\Delta G_{298K,aq}$ and bond lengths at the PCM/B3LYP/6-31+G(d,p)//B3LYP/6-31G(d) level of theory.

Table 1

List of 3,3-, 3,4-, 4,4-, 3,5-, 4,5-, and 5,5-disubstituted nitrones along with generalized structures, categories, and functional groups (R_1 and R_2).

Structure	Category	Entry	R ₁	R ₂	Type ^b
	3,3-Disubstituted	1	-NHC(O)Me	-CO ₂ Me	V
		2	-OMe	-NHMe	
	3,4-Disubstituted ^a	3	-NHC(O)Me	-NHC(O)Me	
		4	-NHC(O)Me	-OMe	
		5	-P(O)(OMe) ₂	-P(O)(OMe) ₂	V
		6	-NHC(O)Me	-P(O)(OMe) ₂	
	4,4-Disubstituted	7	-OMe	-NHMe	
		8	-NHC(O)Me	-P(O)(OMe) ₂	
		9	-NHC(O)Me	-CO ₂ Me	V
		10	-NHC(O)Me	-OMe	
	3,5-Disubstituted ^a	11	-NHC(O)Me	-NHC(O)Me	
		12	-CO ₂ Me	-P(O)(OMe) ₂	
		13	-P(O)(OMe) ₂	-NHC(O)Me	
		14	-P(O)(OMe) ₂	-P(O)(OMe) ₂	
		15	-CO ₂ Me	-NHC(O)Me	I
		16	-P(O)(OMe) ₂	-CO ₂ Me	
		17	-CO ₂ Me	-CO ₂ Me	
		18	-NHC(O)Me	-P(O)(OMe) ₂	
		19	-NHC(O)Me	-CO ₂ Me	

Structure	Category	Entry	R ₁	R ₂	Type ^b
		20	-OMe	-NHC(O)Me	II
		21	-NHMe	-NHC(O)Me	
		22	-NHMe	-P(O)(OMe) ₂	
		23	-OMe	-P(O)(OMe) ₂	
		24	-NHMe	-CO ₂ Me	
		25	-NHC(O)Me	-OMe	III
		26	-P(O)(OMe) ₂	-OMe	
		27	-NHMe	-NHMe	IV
		28	-NHMe	-OMe	
		29	Ester	-P(O)(OMe) ₂	
		30	-P(O)(OMe) ₂	-CO ₂ Me	
		31	-P(O)(OMe) ₂	-NHC(O)Me	
		32	-NHC(O)Me	-NHC(O)Me	I
		33	-NHC(O)Me	Phosphoryl	
		34	-NHC(O)Me	-CO ₂ Me	
		35	-CO ₂ Me	-CO ₂ Me	
		36	-P(O)(OMe) ₂	-P(O)(OMe) ₂	
		37	-CO ₂ Me	-NHC(O)Me	
	4,5-Disubstituted ^a	38	-OMe	-CO ₂ Me	II
		39	-OMe	-P(O)(OMe) ₂	
		40	-NHMe	-P(O)(OMe) ₂	
		41	-OMe	-NHC(O)Me	
		42	-NHMe	-NHC(O)Me	
		43	-NHMe	-CO ₂ Me	
		44	-NHC(O)Me	-OMe	III
		45	-P(O)(OMe) ₂	-OMe	
		46	-OMe	-NHMe	

Structure	Category	Entry	R ₁	R ₂	Type ^b
 5,5-Disubstituted		47	–NHMe	–OMe	IV
		48	–NHMe	–NHMe	
		49	–OMe	–OMe	
		50	–P(O)(OMe) ₂	–CO ₂ Me	I
		51	–P(O)(OMe) ₂	–P(O)(OMe) ₂	
		52	–NHC(O)Me	–CO ₂ Me	
		53	–CO ₂ Me	–CO ₂ Me	
		54	–NHC(O)Me	–P(O)(OMe) ₂	II
		55	–OMe	–CO ₂ Me	
		56	–OMe	–P(O)(OMe) ₂	
		57	–NHMe	–CO ₂ Me	
		58	–NHMe	–P(O)(OMe) ₂	III
		59	–NHC(O)Me	–OMe	
		60	–NHC(O)Me	–NHMe	IV
		61	–OMe	–OMe	
		62	–OMe	–NHMe	
		63	–NHMe	–NHMe	

^aEach nitrone has both *cis*- and *trans*-isomers.

^b(see Table 3) I: EWG at C-5 with additional EWG at either C-3, C-4, or C-5 position, II: EWG at C-5 with additional EDG at either C-3, C-4, or C-5 position, III: EDG at C-5 with additional EWG at either C-3, C-4, or C-5 position, IV: EDG at C-5 with additional EDG at either C-3, C-4, or C-5 position, and V: two methyl groups at C-5.

Table 2

Calculated enthalpies (ΔH_{298K}) and free energies (ΔG_{298K}) in aqueous phase (in kcal/mol) for disubstituted nitron $O_2^{\bullet-}$ and HO_2^{\bullet} adduct formation, as well as nitron C-2 charge densities at the PCM/B3LYP/6-31+G(d,p)/B3LYP/6-31G(d) level of theory.

Substitution	Nitron	C-2 Charge density ^a	$O_2^{\bullet-}$ Spin Adduct ^b		HO_2^{\bullet} Spin Adduct ^b	
			Adduct	ΔH_{298K}	Adduct	ΔH_{298K}
3,3-	1	0.035	1- <i>R-O_2^{\bullet-}</i>	-5.9	1- <i>S-O_2H</i>	-15.1
	2	0.012	2- <i>R-O_2^{\bullet-}</i>	2.0	2- <i>R-O_2H</i>	-12.6
3,4-	3	0.018 (c) 0.026 (t)	3- <i>trans-S-O_2^{\bullet-}</i>	-1.1	3- <i>cis-R-O_2H</i>	-15.0
	4	0.033 (c) 0.022 (t)	4- <i>trans-S-O_2^{\bullet-}</i>	-3.7	4- <i>cis-R-O_2H</i>	-17.8
	5	0.009 (c) 0.001 (t)	5- <i>cis-S-O_2^{\bullet-}</i>	-5.3	5- <i>trans-S-O_2H</i>	-16.3
	6	0.025 (c) 0.020 (t)	6- <i>trans-S-O_2^{\bullet-}</i>	-3.2	6- <i>cis-R-O_2H</i>	-13.6
4,4-	7	0.012	7- <i>R-O_2^{\bullet-}</i>	0.5	7- <i>R-OH</i>	-20.1
	8	0.018	8- <i>S-O_2^{\bullet-}</i>	-3.3	8- <i>S-O_2H</i>	-19.8
	9	0.027	9- <i>R-O_2^{\bullet-}</i>	2.5	9- <i>S-O_2H</i>	-17.8
	10	0.021	10- <i>R-O_2^{\bullet-}</i>	1.5	10- <i>R-O_2H</i>	-11.9
	11	0.062 (c) 0.035 (t)	11- <i>cis-S-O_2^{\bullet-}</i>	-15.3	11- <i>trans-S-O_2H</i>	-20.0
	12	0.051 (c) 0.039 (t)	12- <i>cis-R-O_2^{\bullet-}</i>	-2.4	12- <i>cis-S-O_2H</i>	-20.2
	13	0.052 (c) 0.047 (t)	13- <i>cis-R-O_2^{\bullet-}</i>	-8.5	13- <i>cis-R-O_2H</i>	-16.3
	14	0.030 (c) 0.036 (t)	14- <i>trans-R-O_2^{\bullet-}</i>	-5.6	14- <i>trans-S-O_2H</i>	-18.1
	15	0.062 (c) 0.063 (t)	15- <i>trans-S-O_2^{\bullet-}</i>	-8.9	15- <i>cis-S-O_2H</i>	-16.5
	16	0.012 (c) 0.032 (t)	16- <i>trans-R-O_2^{\bullet-}</i>	-5.8	16- <i>cis-R-O_2H</i>	-15.5
	17	0.042 (c)	17- <i>trans-S-O_2^{\bullet-}</i>	0.3	17- <i>cis-R-O_2H</i>	-16.6

Substitution	Nitrene	C-2 Charge density ^a	O ₂ ^{•-} Spin Adduct ^b			HO ₂ [•] Spin Adduct ^b		
			Adduct	ΔH_{298K}	ΔG_{298K}	Adduct	ΔH_{298K}	ΔG_{298K}
3,5-	18	0.041 (c) 0.044 (t)	18- <i>cis</i> -R-O ₂ ^{•-}	-3.3	9.6	18- <i>trans</i> -R-O ₂ H	-14.8	-3.1
	19	0.036 (c) 0.037 (t)	19- <i>cis</i> -R-O ₂ ^{•-}	-3	6.1	19- <i>trans</i> -R-O ₂ H	-8	-1
	20	0.036 (c) 0.042 (t)	20- <i>trans</i> -S-O ₂ ^{•-}	-0	2.8	20- <i>trans</i> -R-O ₂ H	-3	-3
	21	0.062 (c) 0.059 (t)	21- <i>trans</i> -R-O ₂ ^{•-}	-8	3.2	21- <i>trans</i> -R-O ₂ H	-8	-6
	22	0.039 (c) 0.043 (t)	22- <i>trans</i> -S-O ₂ ^{•-}	-9	10.2	22- <i>cis</i> -R-O ₂ H	-8	-0
	23	0.005 (c) 0.013 (t)	23- <i>cis</i> -R-O ₂ ^{•-}	-7	10.9	23- <i>cis</i> -R-O ₂ H	-0	-9
	24	0.014 (c) 0.033 (t)	24- <i>cis</i> -R-O ₂ ^{•-}	-3	8.1	24- <i>cis</i> -R-O ₂ H	-1	-8
	25	0.029 (c) 0.035 (t)	25- <i>cis</i> -S-O ₂ ^{•-}	-7	7.0	25- <i>cis</i> -R-O ₂ H	-8	-6
	26	0.023 (c) 0.003 (t)	26- <i>cis</i> -S-O ₂ ^{•-}	-4	9.8	26- <i>trans</i> -S-O ₂ H	-3	-3
	27	0.009 (c) 0.019 (t)	27- <i>cis</i> -S-O ₂ ^{•-}	0.4	11.3	27- <i>cis</i> -R-O ₂ H	-6	-4
	28	0.026 (c) 0.032 (t)	28- <i>cis</i> -R-O ₂ ^{•-}	0.7	11.5	28- <i>trans</i> -R-O ₂ H	-1	-1
	29	0.051 (c) 0.042 (t)	29- <i>trans</i> -R-O ₂ ^{•-}	-8	8.2	29- <i>trans</i> -S-O ₂ H	-2	-4
	30	0.038 (c) 0.033 (t)	30- <i>trans</i> -S-O ₂ ^{•-}	0.8	11.0	30- <i>cis</i> -S-O ₂ H	-4	-1
	31	0.033 (c) 0.062 (t)	31- <i>trans</i> -R-O ₂ ^{•-}	-3	3.0	31- <i>cis</i> -R-O ₂ H	-2	-8
	32	0.076 (c) 0.045 (t)	32- <i>cis</i> -S-O ₂ ^{•-}	-8	3.1	32- <i>trans</i> -S-O ₂ H	-2	-4
	33	0.050 (c) 0.055 (t)	33- <i>trans</i> -R-O ₂ ^{•-}	-3	10.4	33- <i>trans</i> -R-O ₂ H	-2	-1
	34	0.038 (c) 0.031 (t)	34- <i>trans</i> -S-O ₂ ^{•-}	-6	6.5	34- <i>trans</i> -S-O ₂ H	-4	-1
	35	0.037 (c) 0.040 (t)	35- <i>cis</i> -R-O ₂ ^{•-}	0.5	10.5	35- <i>trans</i> -R-O ₂ H	-1	-5

Substitution	Nitrene	C-2 Charge density ^a	O ₂ ^{•-} Spin Adduct ^b			HO ₂ [•] Spin Adduct ^b		
			Adduct	ΔH_{298K}	ΔG_{298K}	Adduct	ΔH_{298K}	ΔG_{298K}
4,5-	36	0.044 (c) 0.053 (t)	36- <i>trans</i> -S-O ₂ ^{•-}	-2	11.5	36- <i>cis</i> -S-O ₂ H	-3	-3
	37	0.066 (c) 0.066 (t)	37- <i>trans</i> -S-O ₂ ^{•-}	-4	7.4	37- <i>cis</i> -S-O ₂ H	-9	-2
	38	0.040 (c) 0.033 (t)	38- <i>cis</i> -S-O ₂ ^{•-}	-3	9.9	38- <i>cis</i> -S-O ₂ H	-1	-3
	39	0.037 (c) 0.046 (t)	39- <i>trans</i> -R-O ₂ ^{•-}	-4	11.4	39- <i>trans</i> -R-O ₂ H	-8	-5
	40	0.048 (c) 0.044 (t)	40- <i>trans</i> -S-O ₂ ^{•-}	-8	8.7	40- <i>trans</i> -R-O ₂ H	-0	-3
	41	0.041 (c) 0.059 (t)	41- <i>cis</i> -R-O ₂ ^{•-}	-8	0.1	41- <i>cis</i> -S-O ₂ H	-8	-3
	42	0.071 (c) 0.063 (t)	42- <i>trans</i> -S-O ₂ ^{•-}	-5	5.4	42- <i>cis</i> -R-O ₂ H	-3	-9
	43	0.041 (c) 0.035 (t)	43- <i>cis</i> -S-O ₂ ^{•-}	0.0	10.3	43- <i>cis</i> -S-O ₂ H	-7	-2
	44	0.039 (c) 0.023 (t)	44- <i>trans</i> -R-O ₂ ^{•-}	-0	7.4	44- <i>trans</i> -S-O ₂ H	-7	-3
	45	0.032 (c) 0.039 (t)	45- <i>trans</i> -R-O ₂ ^{•-}	-9	11.8	45- <i>cis</i> -R-O ₂ H	-5	-7
	46	0.024 (c) 0.033 (t)	46- <i>trans</i> -R-O ₂ ^{•-}	-2	8.7	46- <i>trans</i> -S-O ₂ H	-7	-7
	47	0.037 (c) 0.028 (t)	47- <i>trans</i> -R-O ₂ ^{•-}	0.1	11.3	47- <i>cis</i> -R-O ₂ H	-7	-8
	48	0.037 (c) 0.019 (t)	48- <i>cis</i> -S-O ₂ ^{•-}	2.1	12.7	48- <i>cis</i> -S-O ₂ H	-0	-0
	49	0.028 (c) 0.028 (t) 0.058	49- <i>trans</i> -R-O ₂ ^{•-} -50-S-O ₂ ^{•-}	-5 -7	9.7 7.5	49- <i>cis</i> -S-O ₂ H 50-S-O ₂ H	-7 -5	-2
	50							-1
	51	0.063	51-R-O ₂ ^{•-}	-0	8.7	51-R-O ₂ H	-1	-0
	52	0.072	52-S-O ₂ ^{•-}	-2	6.9	52-R-O ₂ H	-7	-5
	53	0.043	53-R-O ₂ ^{•-}	3.8	15.5	53-R-O ₂ H	-8	-4
	54	0.080	54-R-O ₂ ^{•-}	-6	5.4	54-S-O ₂ H	-7	-2

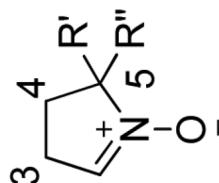
Substitution	Nitron	C-2 Charge density ^a	O ₂ ^{•-} Spin Adduct ^b			HO ₂ [•] Spin Adduct ^b		
			Adduct	ΔH_{298K}	ΔG_{298K}	Adduct	ΔH_{298K}	ΔG_{298K}
5,5-	55	0.048	55- <i>R</i> -O ₂ ^{•-}	-6	8.7	55- <i>S</i> -O ₂ H	-5	-9
	56	0.060	56- <i>R</i> -O ₂ ^{•-}	1.2	10.5	56- <i>S</i> -O ₂ H	-2	-7
	57	0.030	57- <i>R</i> -O ₂ ^{•-}	3.2	14.6	57- <i>S</i> -O ₂ H	-7	-6
	58	0.058	58- <i>R</i> -O ₂ ^{•-}	-8	10.0	58- <i>S</i> -O ₂ H	-1	-0
	59	0.057	59- <i>R</i> -O ₂ ^{•-}	-0	10.2	59- <i>R</i> -O ₂ H	-0	-5
	60	0.044	60- <i>R</i> -O ₂ ^{•-}	-1	8.8	60- <i>S</i> -O ₂ H	-4	-0
	61	0.043	61- <i>S</i> -O ₂ ^{•-}	-7	8.1	61- <i>S</i> -O ₂ H	-4	-5
	62	0.044	62- <i>R</i> -O ₂ ^{•-}	-6	10.8	62- <i>R</i> -O ₂ H	-5	-4
	63	0.024	63- <i>S</i> -O ₂ ^{•-}	-7	7.3	63- <i>S</i> -O ₂ H	-7	-7

^a the letters “c” and “t” in parentheses stand for *cis* and *trans* respectively.

^b only shown in this column are the spin adducts with the most favorable $\Delta G_{298K,aq}$ among all isomeric spin adducts calculated for each nitron.

Table 3

Various categories of disubstituted nitrones according to the nature (i.e., EDG or EWG) and the position (i.e., C-3, C-4 and C-5) of the substituents.



Type I	Type II	Type III	Type IV	Type V
C-3 EWG	EDG	EWG	EDG	EDG and/or EWG
C-4 EWG	EDG	EWG	EDG	EDG and/or EWG
C-5 EWG	EWG	EDG	EDG	none

Table 4

Calculated enthalpies ($\Delta H_{298K,aq}$) and free energies ($\Delta G_{298K,aq}$) in kcal/mol, and other parameters for the complexes, TS structures, and spin adducts for the $O_2^{\bullet-}$ and HO_2^{\bullet} additions to **11-*cis*** and **29-*trans***, respectively, at the PCM/B3LYP/6-31+G(d,p)//B3LYP/6-31G(d) level of theory.

Structure	$\Delta H_{298K,aq}$	$\Delta G_{298K,aq}$	C...O ₂ ^{•-} [Å]	$\langle S^2 \rangle$	Imaginary frequency ^e
<i>11-cis</i>					
11-<i>cis</i> + O ₂ ^{•-} ^a	0	0	∞	0	0
11-<i>cis</i> ...O ₂ ^{•-} ^b	-5.2	2.6	2.97	0.76	0
[11-<i>cis</i> :O ₂ ^{•-}] ^{†c}	1.8	14.4	1.80	0.78	570i
11-<i>cis</i> -S-O ₂ ^{•-} ^d	-15.3	-3.3	1.39	0.75	0
<i>29-trans</i>					
29-<i>trans</i> + HO ₂ ^{•a}	0	0	∞	0	0
29-<i>trans</i> ...HO ₂ ^{•b}	-5.0	5.4	3.17	0.75	0
[29-<i>trans</i> :O ₂ H] ^{†c}	2.5	15.7	2.10	0.79	415i
29-<i>trans</i> -R-O ₂ H ^d	-21.2	-9.4	1.40	0.75	0

^a At infinite separation

^b Complex

^c Transition state

^d Product

^e Only one imaginary frequency was observed in the TS structure (in cm⁻¹).